The EMBO Journal Vol. 21 No. 24 pp. 6733–6743, 2002

Glycerotoxin from *Glycera convoluta* stimulates neurosecretion by up-regulating N-type Ca^{2+} channel activity

Frédéric A.Meunier[1,2,3], Zhong-Ping Feng[4], Jordi Molgó[5], Gerald W.Zamponi[4] and Giampietro Schiavo[1,3]

[1]Molecular Neuropathobiology Laboratory, Cancer Research UK, London Research Institute, Lincoln's Inn Fields Laboratories, 44 Lincoln's Inn Fields, London WC2A 3PX, UK, [4]Department of Physiology and Biophysics, University of Calgary, 3330 Hospital Drive NW, Calgary T2N 4N1, Canada and [5]Laboratoire de Neurobiologie Cellulaire et Moleculaire, UPR 9040, CNRS, 1 avenue de la Terrasse, 91198 Gif-sur-Yvette, France

[2]Present address: MRC Laboratory of Molecular Biology, Hills Road, Cambridge CB2 2QH, UK

[3]Corresponding authors
e-mail: fmeunier@mrc-lmb.cam.ac.uk or giampietro.schiavo@cancer.org.uk

We report here the purification of glycerotoxin from the venom of *Glycera convoluta*, a novel 320 kDa protein capable of reversibly stimulating spontaneous and evoked neurotransmitter release at the frog neuromuscular junction. However, glycerotoxin is ineffective at the murine neuromuscular junction, which displays a different subtype of voltage-dependent Ca^{2+} channels. By sequential and selective inhibition of various types of Ca^{2+} channels, we found that glycerotoxin was acting via $Ca_v2.2$ (N-type). In neuroendocrine cells, it elicits a robust, albeit transient, influx of Ca^{2+} sensitive to the $Ca_v2.2$ blockers ω-conotoxin GVIA and MVIIA. Moreover, glycerotoxin triggers a Ca^{2+} transient in human embryonic kidney (HEK) cells over-expressing $Ca_v2.2$ but not $Ca_v2.1$ (P/Q-type). Whole-cell patch–clamp analysis of $Ca_v2.2$ expressing HEK cells revealed an up-regulation of Ca^{2+} currents due to a leftward shift of the activation peak upon glycerotoxin addition. A direct interaction between $Ca_v2.2$ and this neurotoxin was revealed by co-immunoprecipitation experiments. Therefore, glycerotoxin is a unique addition to the arsenal of tools available to unravel the mechanism controlling Ca^{2+}-regulated exocytosis via the specific activation of $Ca_v2.2$.

Keywords: Ca^{2+} channels/exocytosis/glycerotoxin/neuromuscular junction/neurotoxin

Introduction

Milestones in our understanding of synaptic functions have been reached using naturally occurring neurotoxins. Fashioned by billions of years of evolution and struggle for life between competing species, neurotoxins have the ability to incapacitate prey by interfering with synaptic processes at strategic points. This arms race has had beneficial scientific outcomes. Indeed, neurotoxins directly affecting neurotransmitter release have been used as tools for deciphering several aspects of exo- and endocytosis and to characterize the role of many of the proteins involved in these processes (Schiavo *et al*., 2000).

The sea worms *Glycera convoluta* (Figure 1A) are polychaete annelids which live in burrows on the shoreline of coastal regions and are highly active carnivorous predators. They detect their prey, mostly crustaceans and other polychaetes, by sensing hydrostatic changes and attack by shooting out an eversible proboscis (Figure 1B). The latter unveils four chitinous copper-containing fangs (Lichtenegger *et al*., 2002) used to inject their prey with its deadly venom. In the early 1980s, this venom was studied because of its ability to stimulate spontaneous quantal acetylcholine (ACh) release at the frog neuromuscular junction (NMJ) (Manaranche *et al*., 1980). The venom produces a prolonged but fully reversible high-frequency discharge of miniature end-plate potentials (MEPPs) without altering the ultrastructural features of the NMJ. For these reasons, the active compound is expected to be an invaluable tool for studying the regulation of synaptic vesicle recycling. Early attempts to purify the active component of the venom suggested that the biological activity was linked to a high-molecular-weight glycoprotein (Morel *et al*., 1983). However, to date, no further attempts have been made to isolate the toxin, to identify its receptor or to decipher its mode of action.

Herein, the successful purification and characterization of an active 320 kDa glycoprotein called glycerotoxin (GLTx) is reported. Using a strategy based on the pharmacology of voltage-dependent Ca^{2+} channels (VDCCs), $Ca_v2.2$ (N-type Ca^{2+} channel) has been identified as the presynaptic target of GLTx. Notably, $Ca_v2.2$ channels are one of the main presynaptic Ca^{2+} channels involved in fast neurotransmitter release. They are assembled by the association of the channel-forming subunit α_{1B} with the auxiliary subunits β and α_2–δ, which act as modulators. $Ca_v2.2$ interacts, via a region of α_{1B} called synprint, with members of the exocytotic apparatus allowing a tight control of vesicular release (Catterall, 2000; Jarvis and Zamponi, 2001).

GLTx elicits a transient Ca^{2+} influx sensitive to selective blockers of $Ca_v2.2$ in chromaffin cells and in human embryonic kidney cells (HEK293) over-expressing $Ca_v2.2$. Patch–clamp analysis showed that, upon addition of GLTx, the current–voltage relationship was shifted towards more hyperpolarized potentials promoting an up-regulation of current activity. This prompted us to investigate the effect of GLTx on nerve-evoked synchronous transmitter release, which revealed a sustained potentiation of phasic secretion. Finally, co-immunoprecipitation experiments showed that $Ca_v2.2$ was selectively

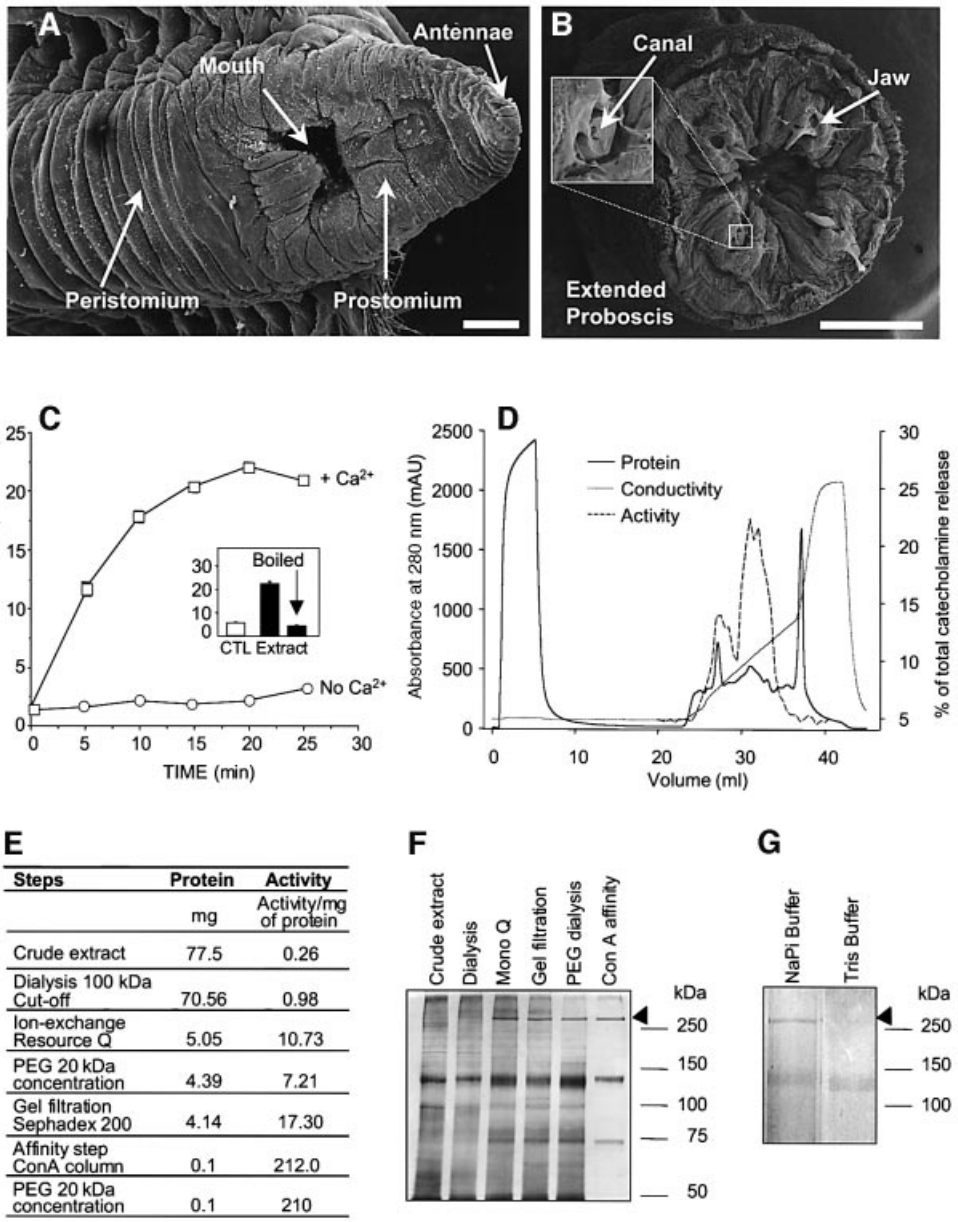

Steps	Protein	Activity
	mg	Activity/mg of protein
Crude extract	77.5	0.26
Dialysis 100 kDa Cut-off	70.56	0.98
Ion-exchange Resource Q	5.05	10.73
PEG 20 kDa concentration	4.39	7.21
Gel filtration Sephadex 200	4.14	17.30
Affinity step ConA column	0.1	212.0
PEG 20 kDa concentration	0.1	210

Fig. 1. Purification of the secretagogue activity from *G.convoluta* venom. Scanning electron micrographs of the head (**A**) and the terminal tip of the proboscis of *G.convoluta* showing the four chitinous fangs (**B**) connected with the venomous glands via a duct. The proboscis can be thrust outward in a fast contractile motion, allowing the worm to bite its prey and inject venom. Scales: 500 μm. (**C**) Chromaffin cells bathed in buffer A in the presence (squares) or absence (circles) of 2 mM Ca^{2+} were exposed for the indicated periods to the crude gland extract (0.17 mg/ml) before assaying catecholamine secretion, expressed as a percentage of the total catecholamine content of the cells (± SEM; $n = 4$). Insert: catecholamine secretion from chromaffin cells exposed for 20 min to boiled or unboiled crude venom (0.17 mg/ml) in the presence of 2 mM Ca^{2+} (filled bars). (**D**) Chromatogram of a dialysed extract from 200 homogenized glands applied on an anion-exchange Resource Q matrix. Fractions were eluted with a gradient of 0–1 M NaCl in 50 mM sodium phosphate (pH 7.4) (broken line). Each fraction was tested for its ability to trigger catecholamine secretion from chromaffin cells (hatched line) as described above. Proteins eluted in the void volume lack any stimulatory activity whereas the two peaks eluted at 100 and 300 mM NaCl exhibited a secretagogue activity. Specific activity of GLTx (**E**) and silver-stained SDS–PAGE profile (**F**) at different stages of purification (5 μg protein per lane). (**G**) The Con A-affinity-purified fraction was split and incubated for 1 h at room temperature in the presence or absence of Tris–HCl buffer (50 mM final, pH 8.0) prior to SDS–PAGE and silver staining.

recovered from brain synaptosomes in a complex with GLTx.

By specifically interacting with $Ca_v2.2$, GLTx represents a novel major tool with great potential to elucidate the role of $Ca_v2.2$ in a wide range of neuronal processes in both the central nervous system (CNS) and the peripheral nervous system (PNS).

Results

Purification of a secretagogue component from the venomous glands of the sea worm Glycera convoluta

To follow the purification of the secretagogue component from the venomous glands of *G.convoluta*, we have tested

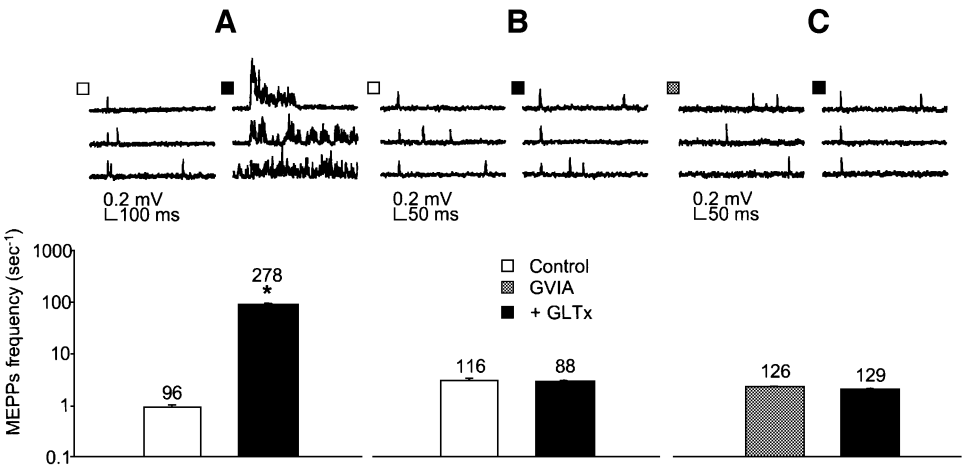

Fig. 2. Differential effect of GLTx on frog and murine NMJ. Intracellular recording of spontaneous quantal ACh release from frog (A and C) and mouse (B) neuromuscular preparations, in a Ca^{2+}-containing Ringer solution before (empty bars) and after (filled bars) application of 0.1 μg/ml GLTx. Sampled traces were collected and analysed for mean MEPP frequency 5 min before and 10–20 min after adding GLTx, and characteristic examples are shown (upper panels). Note the massive increase in MEPP frequency observed at frog NMJs (**A**). In contrast, no modification of MEPP frequency was detectable in mouse EDL preparation following application of 0.1 μg/ml GLTx (**B**). Pre-treatment of the frog NMJ with ω-CTx-GVIA (1 μM, 20 min) totally prevented GLTx-induced rise in MEPPs frequency (**C**). The number of sampled traces analysed for quantifying the mean MEPP frequency is indicated. Plotted values are representative of at least three independent experiments.

the ability of the venom to elicit catecholamine release from primary monolayer cultures of bovine chromaffin cells by fluorimetry (Meunier *et al*., 2000). Following the homogenization of the venomous glands (Figure 1B), chromaffin cells were exposed to the extract (0.3 mg/ml), which induced the release of ~20% of their total catecholamine content with maximal secretion reached after 20 min (Figure 1C). This response was Ca^{2+} dependent as no stimulatory effect was observed in the absence of external Ca^{2+} (Figure 1C). This activity was lost after heating the extract at 100°C for 5 min (Figure 1C, insert), suggesting that the secretagogue could be a protein. Having established that these primary neurosecretory cells were suitable for testing fractions from the venom, we undertook the purification of the active component using bovine chromaffin cells as a functional assay. Previous studies have reported the partial purification of an active fraction, devoid of lipolytic or proteolytic activities, containing, among several other contaminants, a protein with an apparent molecular weight of 300 kDa (Morel *et al*., 1983). Therefore, the initial purification step was to clear the crude extract from low-molecular-weight proteins using a 100 kDa cut-off dialysis membrane. As expected, the dialysed material was still stimulating catecholamine release from chromaffin cells (Figure 1E). The active component was further purified using ion-exchange chromatography (Figure 1D). Interestingly, a 320 kDa band could clearly be observed on a silver-stained gel of the eluted fractions, exhibiting an ~10-fold increase in the specific activity (Figure 1E and F). The active pool was concentrated, desalted and further purified by gel filtration, which achieved a doubling in the specific activity of the partially purified extract (Figure 1E and F). Finally, the neurotoxin was affinity purified using the known ability of the active component of the venom to bind concanavalin A (Con A) (Morel *et al*., 1983). This last step reduced the complexity of the purified fraction to three proteins: a 320 kDa band, a 148 kDa band and a 74 kDa band which was not always detectable (Figure 1F). Henceforth, this final fraction will be referred to as purified glycerotoxin. Based on the comparison of several purifications using the same or similar protocols, the activity of the purified neurotoxin clearly followed the distribution pattern of the 320 kDa band. Moreover, treatment of glycerotoxin for 1 h at pH 8.0 at room temperature in Tris buffer (50 mM) causes the selective disappearance of the 320 kDa band (Figure 1G), which is paralleled by an abolition of the secretagogue activity (data not shown). In these conditions the 148 kDa band remained unaffected, indicating that the active component of the venom is the 320 kDa protein (Figure 1G). In the presence of 2-mercaptoethanol, the 320 and 148 kDa proteins exhibit a decrease in their mobility to 335 and 176 kDa, respectively, suggesting that one or more internal disulphide bridges might affect the overall shape and mobility of the protein (data not shown). Peptide mass fingerprinting analysis indicates that the 320 kDa component does not correspond to any entry present in the DDBJ/EMBL/GenBank protein database (http://www.ncbi.nlm.nih.gov/BankIt), suggesting that GLTx is a novel protein.

GLTx increases spontaneous quantal ACh release at frog but not mouse neuromuscular junctions

The activity of GLTx was subsequently tested at the frog NMJ using the cutaneous pectoris muscle upon which the venom enhances spontaneous quantal transmitter release (Manaranche *et al*., 1980). At the frog NMJ, 0.05–0.3 μg/ml of purified GLTx markedly enhanced spontaneous quantal transmitter release after only a few minutes delay, as detected by a sustained increase in the frequency of MEPPs (Figure 2A). To determine whether GLTx has similar effects on a mammalian NMJ, we tested it on the mouse extensor digitorum longus (EDL) nerve–muscle preparation. Interestingly, in this preparation,

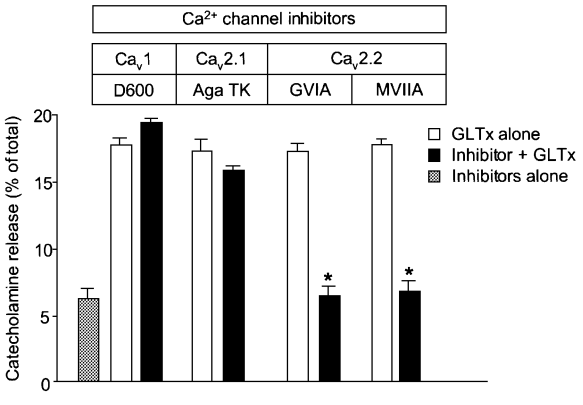

Fig. 3. GLTx-induced catecholamine release is prevented by preincubation with $Ca_v2.2$ but not $Ca_v2.1$ or Ca_v1 blockers. Primary cultures of adrenal chromaffin cells were pre-incubated for 15 min in the absence (open bars) or the presence (filled bars) of selective inhibitors of VDCC (100 μM D600; 1 μM Aga TK; 2 μM ω-CTx-GVIA and ω-CTx-MVIIA) before adding GLTx (0.2 μg/ml) for another 20 min in a Ca^{2+}-containing buffer A. Aliquots were assayed fluorimetrically for catecholamine release and the evoked secretion expressed as a percentage of total catecholamine content. Data showing the basal release of unstimulated cells exposed for 35 min to any of the above-mentioned inhibitors were pooled (grey bar).

GLTx (0.05–10 μg/ml) was totally ineffective in modifying quantal spontaneous transmitter release (Figure 2B).

Therefore, we investigated established differences between the murine and frog components of the motor nerve terminals that could underlie such a discrepancy. Frog motor nerve terminals mainly contain $Ca_v2.2$ (Robitaille *et al*., 1990), whereas murine endplates express mainly $Ca_v2.1$ (Day *et al*., 1997; Katz *et al*., 1997). As both $Ca_v2.2$ and $Ca_v2.1$ interact with the secretory apparatus in neurons, a plausible explanation for the stimulatory effect of GLTx at the frog versus the mouse NMJ is that GLTx selectively acts on $Ca_v2.2$.

To test this hypothesis, frog neuromuscular preparations were pre-treated with ω-conotoxin-GVIA (ω-CTx-GVIA), a selective inhibitor of $Ca_v2.2$ (Olivera *et al*., 1985, 1999). Notably, this procedure abolishes the increase in asynchronous quantal ACh release in response to GLTx application, strongly implicating $Ca_v2.2$ as a target for GLTx (Figure 2C).

GLTx stimulates catecholamine release from bovine chromaffin cells by causing a transient influx of Ca^{2+} sensitive to $Ca_v2.2$ selective inhibitors

Bovine chromaffin cells are known to express Ca_v1, $Ca_v2.2$ and $Ca_v2.1$ (Artalejo *et al*., 1994; Garcia *et al*., 1998) and therefore provide an excellent model to pinpoint the subtype of VDCC involved in GLTx action. Pre-treatment of chromaffin cells with D600, a Ca_v1 blocker, or Agatoxin TK (Aga TK), a $Ca_v2.1$ blocker, thereby sparing $Ca_v2.2$, was unable to prevent the secretagogue activity of GLTx (Figure 3). However, the specific inhibition of $Ca_v2.2$ using ω-CTx-GVIA or ω-CTx-MVIIA (Olivera *et al*., 1985, 1999) blocked catecholamine secretion evoked by GLTx (Figure 3). These results demonstrate that GLTx stimulates catecholamine-containing secretory granule exocytosis by targeting $Ca_v2.2$.

Since Ca^{2+} is a general trigger for regulated exocytosis and the secretagogue activity of GLTx is strictly dependent upon the presence of external Ca^{2+} in chromaffin cells, we tested whether GLTx stimulates secretion by increasing intracellular Ca^{2+} as a result of a functional interaction with $Ca_v2.2$. To test this hypothesis, chromaffin cells were loaded with the Ca^{2+}-sensitive dyes fura-2 or fluo-3. In the presence of Ca^{2+} in the external medium, application of GLTx (0.1–1.0 μg/ml) transiently increased intracellular Ca^{2+} (Figure 4A and B). Importantly, in an external medium devoid of Ca^{2+}, addition of GLTx did not trigger any detectable Ca^{2+} rise (Figure 4C). However, subsequent addition of Ca^{2+} (2 mM) in the GLTx-containing medium resulted in a transient increase in intracellular Ca^{2+} (Figure 4C). These results demonstrate that GLTx triggers an influx of Ca^{2+} able to trigger catecholamine secretion from chromaffin cells.

To verify that this rise in intracellular Ca^{2+} signal was initiated by a GLTx-dependent influx through $Ca_v2.2$, we used selective inhibitors to block the different types of VDCC present in chromaffin cells before applying GLTx. Blockade of Ca_v1 with D600 (100 μM) did not significantly affect the GLTx-induced Ca^{2+} transient (Figure 4D). Similarly, pre-treatment with Aga TK (1 μM), a $Ca_v2.1$ blocker, was unable to block this effect (Figure 4D).

In contrast, when chromaffin cells were monitored in the presence of ω-CTx-MVIIA (2 μM), a reversible $Ca_v2.2$ blocker, GLTx application did not result in any detectable increase in Ca^{2+} (Figure 4E). Interestingly, when the same cells were washed and monitored again, application of GLTx alone was capable of eliciting an increase in intracellular Ca^{2+} (Figure 4E). Altogether, these results demonstrated that $Ca_v2.2$ is necessary for GLTx to trigger an influx of Ca^{2+} and to stimulate catecholamine neurosecretion from chromaffin cells.

GLTx triggers an influx of Ca^{2+} in human embryonic kidney cells transiently transfected with $Ca_v2.2$ but not with $Ca_v2.1$

To examine whether the presence of $Ca_v2.2$ is sufficient for GLTx to trigger Ca^{2+} influx, we used the heterologous HEK cell system transiently transfected with either $Ca_v2.2$ or $Ca_v2.1$. The expression of $Ca_v2.2$ and $Ca_v2.1$ on the plasma membrane was checked by immunocytochemistry (data not shown). After establishing that the intracellular Ca^{2+} level in untransfected cells was not affected by GLTx (0.1–1.0 μg/ml) (not shown), we over-expressed various subunits encoding $Ca_v2.2$ or $Ca_v2.1$. Only cells over-expressing the $Ca_v2.2$ subunits α_{1B} in the presence of β subunit (± α_2–δ) responded to the application of GLTx with a robust transient intracellular Ca^{2+} signal (Figure 5, insert). Moreover, pre-incubation of HEK cells expressing $Ca_v2.2$ with ω-CTx-GVIA totally prevented this Ca^{2+} signal (Figure 5, grey bar and insert). To show that GLTx was acting on $Ca_v2.2$ exposed on the plasma membrane, HEK cells were transfected with α_{1B} subunit only. β_3 is required to overcome an endoplasmic reticulum (ER) retention signal present in the α_1 subunit, and failure to co-express β subunit results in a lack of expression of the channel at the plasma membrane (Walker and De Waard, 1998; Bichet *et al*., 2000). These cells were insensitive to GLTx, clearly demonstrating that the toxin acts extra-

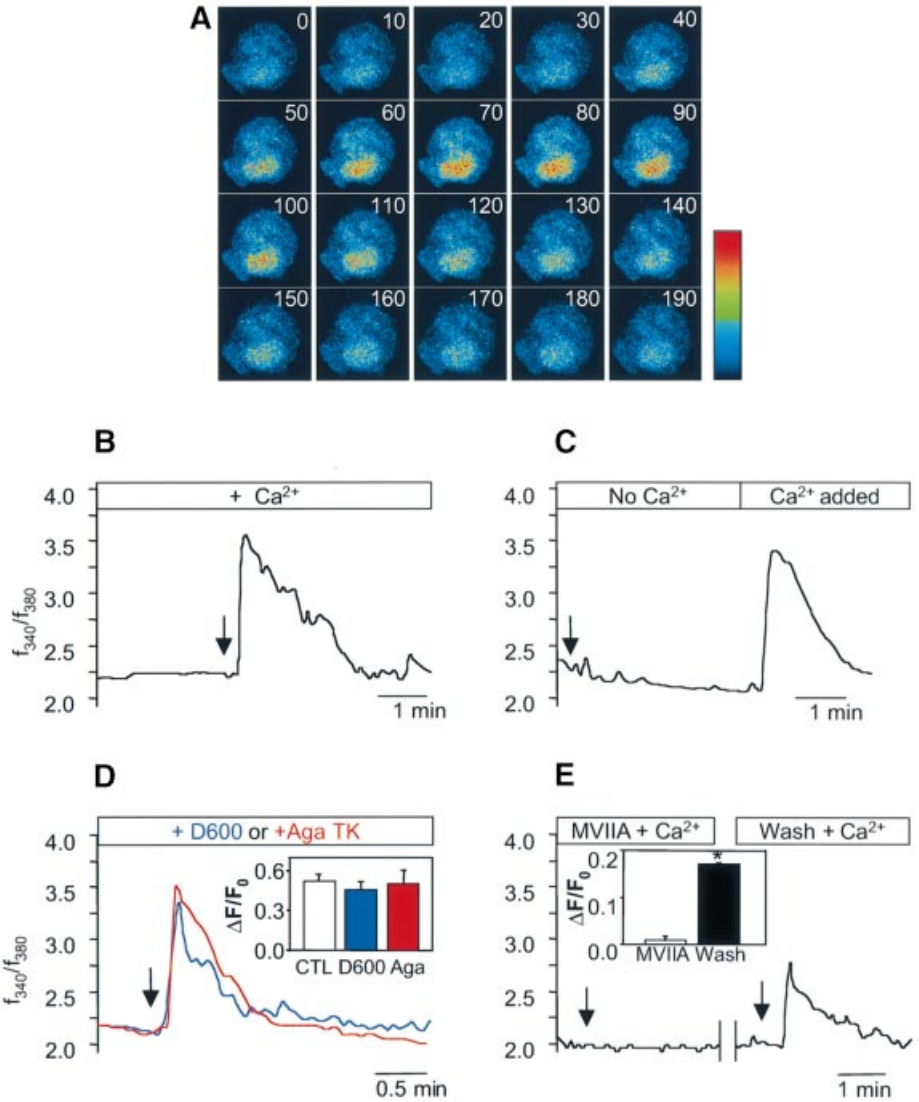

Fig. 4. GLTx induces an influx of Ca^{2+} in chromaffin cells sensitive to $Ca_v2.2$ blockers. (**A**) Series of confocal images acquired at 10 s intervals of a fluo-3-labelled chromaffin cell treated with GLTx (0.1 μg/ml) at $t = 20$ s in the presence of Ca^{2+}. (B–E) Time-course of changes in the ratio of fluorescent signals of fura-2-loaded chromaffin cells exposed to 0.1 μg/ml GLTx. Arrows indicate the time of GLTx application. (**B**) Cells were treated with GLTx in the presence of external Ca^{2+}. (**C**) Cells were pre-incubated with GLTx in the absence of Ca^{2+} prior to addition of 2 mM Ca^{2+}. (**D**) GLTx was applied following pre-incubation for 15 min with 100 μM D600 (blue line) or 1 μM Aga TK (red line). Insert: quantification of the maximum amplitudes of intracellular Ca^{2+} variations evoked by GLTx in control cells (empty bar; $n = 30$) or in the presence of D600 (blue bar; $n = 25$) or Aga TK (red bar; $n = 15$). (**E**) Cells were incubated with ω-CTx-MVIIA (2 μM) for 15 min before application of GLTx in the presence of Ca^{2+}. The same cells were quickly washed in a toxin-free buffer and subsequently re-exposed to GLTx alone. Insert: quantification of the maximum amplitudes of intracellular Ca^{2+} variations evoked by GLTx in the presence (open bar; $n = 7$) or after washing out (filled bar; $n = 7$) of ω-CTx-MVIIA.

cellularly on $Ca_v2.2$ present on the plasma membrane (Figure 5). Importantly, the level of Ca^{2+} in response to GLTx exposure remained unaffected in HEK cells transfected with α_{1A} ($\pm$ β_3 $\pm$ α_2–δ) encoding $Ca_v2.1$.

Anti-GLTx monoclonal antibodies co-immunoprecipitate $Ca_v2.2$

To investigate a possible direct interaction between GLTx and $Ca_v2.2$, GLTx-interacting proteins were co-immunoprecipitated from solubilized rat brain membranes (LP1) using a monoclonal antibody against purified GLTx. In the screening procedure, we selected a positive clone, named 4G9, which recognized purified GLTx on dot-blot (Figure 6A) and was able to immunoprecipitate GLTx from both the purified GLTx (Figure 6B) and crude extract (data not shown). In western blotting, 4G9 antibodies recognized not only the 320 kDa band specific for the active toxin (Figure 6B) but also the 148 kDa band, suggesting that the latter is a degradation product of the former (data not shown).

Immunoprecipitation of GLTx followed by incubation with solubilized rat brain membranes led to the specific recovery of $Ca_v2.2$ as evidenced by probing for the α_{1B} subunit in western blotting (Figure 6C). Moreover, co-immunoprecipitation revealed that GLTx could pull down up to 25% of the total [^{125}I]ω-CTx-GVIA binding sites corresponding to α_{1B} from detergent extracts of rat brain membranes (Figure 6D). These results confirm

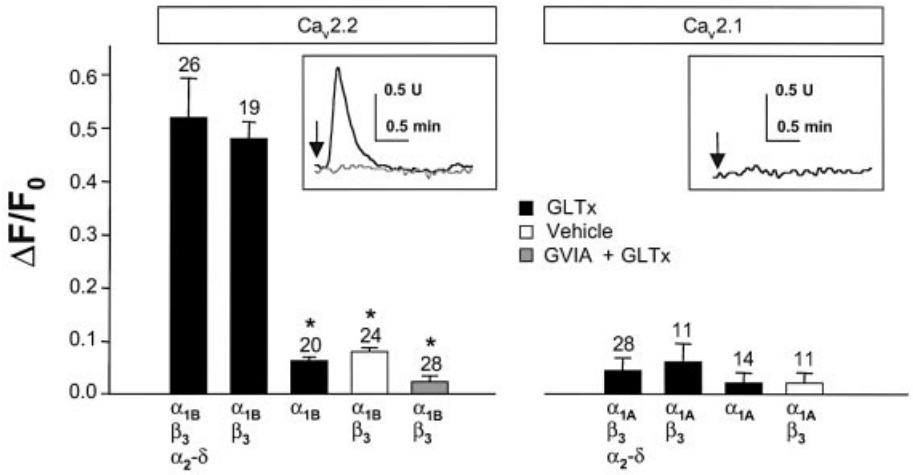

Fig. 5. Expression of $Ca_v2.2$ in HEK cells confers sensitivity to GLTx. HEK cells were transfected with various combinations of expression vectors encoding the different subunits of $Ca_v2.2$ or $Ca_v2.1$, as indicated on the figure, before fura-2 loading. Cells were monitored for intracellular Ca^{2+} variations (see insert) during GLTx (0.1 μg/ml) exposure (black lines and filled bars) or vehicle (open bars). Bars show the quantitation of the amplitudes of the Ca^{2+} transients (0.1 μg/ml) in medium containing 2 mM Ca^{2+}. Note that the Ca^{2+} signal induced by GLTx in HEK cells expressing $Ca_v2.2$ is totally prevented by pre-incubation for 15 min with 2 μM ω-CTx-GVIA (grey bar and grey line in the insert). The number of transfected cells examined is indicated on the top of the bars.

biochemically the specificity of the interaction between GLTx and $Ca_v2.2$.

Patch–clamp analysis of the action of GLTx

Whole-cell patch–clamp recordings were carried out on N-type Ca^{2+} channels (α_{1B} + α_2–δ + β_{2a}) transiently expressed in HEK tsA-201 cells. At depolarized potentials, a small reduction in the maximum slope conductance could be observed, resulting in current inhibition at positive potentials (Figure 7A and C). Importantly, GLTx (0.03 μg/ml) significantly shifted the current–voltage relationship to more hyperpolarized potentials by about 10 mV. Hence, at hyperpolarized test potentials, GLTx promotes an up-regulation of current activity resulting in a large increase in peak current amplitude when test potential is stepped to –10 mV (Figure 7A, B and C). The enhanced inward current was slowly reversible and could be blocked by subsequent application of ω-CTx-MVIIA, indicating that it resulted from an up-regulation of N-type channel activity (Figure 7B, insert).

The 10 mV shift in half activation potential produced by GLTx is irrespective of the nature of the β subunit (Figure 7D). Moreover, as in the case of β_{2a} (see Figure 7A), a small degree of inhibition was observed at more depolarized potentials when the other three β subunits were co-expressed (not shown). Given the similar shifts in half activation potential, a similar level of up-regulation of current activity could be predicted at negative test potentials, and was indeed observed (Figure 7E). GLTx did not significantly affect the voltage dependence of inactivation for channels containing the β_{1b} or β_{2a} subunit ($n = 4$, not shown). At higher concentrations (0.25 μg/ml), GLTx almost completely inhibited N-type channel activity (data not shown). This might indicate that GLTx has two separate sites of action on the N-type channel molecule: one high affinity linked to changes in gating properties, and a second low affinity that results in block of current activity.

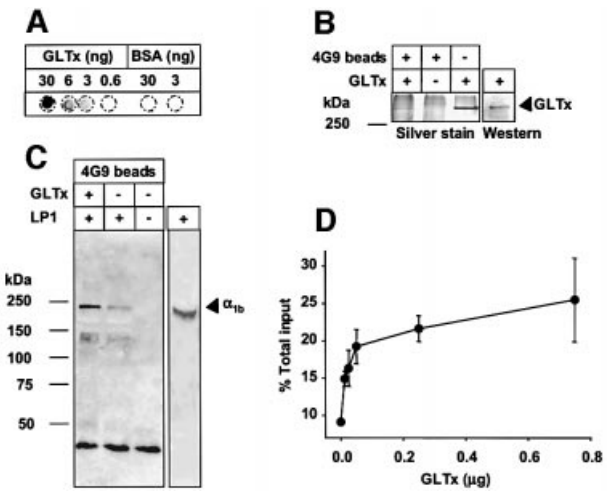

Fig. 6. The α_{1B} subunit of $Ca_v2.2$ interacts with GLTx. (**A** and **B**) Characterization of the monoclonal antibody 4G9 raised against GLTx. The monoclonal antibody 4G9 recognizes purified GLTx in a dot-blot assay in a dose-dependent manner (A). In western blotting, this antibody recognizes the 320 kDa band and it is able to immunoprecipitate native GLTx (B). 4G9-coated or uncoated Protein G–Sepharose beads were incubated for 1 h in the presence or absence of purified GLTx, washed, run on a 12% SDS–PAGE and silver stained (B). The 320 kDa band corresponding to GLTx is recovered in the immunoprecipitate. (**C**) 4G9-coated Protein G–Sepharose beads were incubated for 1 h in the presence or absence of purified GLTx, washed and incubated in the presence or absence of detergent-solubilized rat brain membrane extract (LP1). The bound material was washed, separated in 12% SDS–PAGE, transferred onto nitrocellulose membrane and probed with an antibody against the α_{1B} subunit of $Ca_v2.2$. One-fifth of the membrane extract used in the immunoprecipitation was also loaded (C, right lane). (**D**) 4G9-coated Protein G–Sepharose beads were incubated for 1 h in the presence of increasing amount of GLTx (amount added indicated in the figure), washed and incubated with solubilized rat brain membrane extract pre-labelled with [I^{125}]ω-CTx-GVIA. Pull-down material was counted and expressed as a percentage of the total input.

Therefore, taken together, our data suggest that the size of the window current is increased in the presence of GLTx, thus leading to increased Ca^{2+} influx.

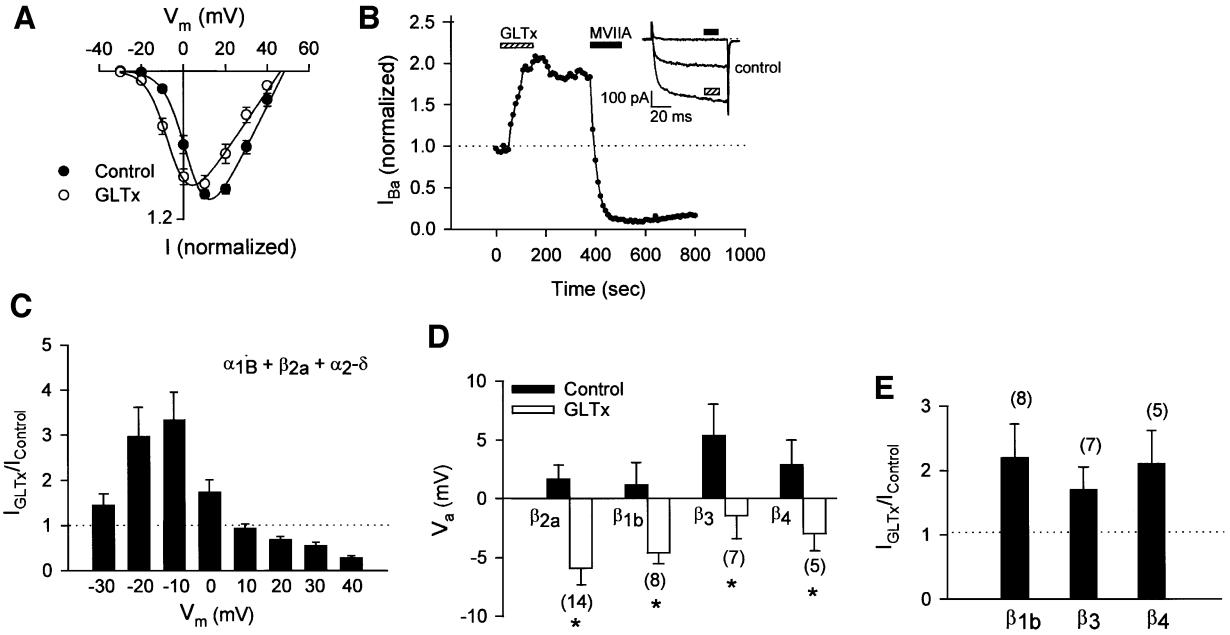

Fig. 7. Electrophysiological characterization of the effects of GLTx on N-type Ca^{2+} channels transiently expressed in HEK tsA-201 cells. (**A**) Ensemble current–voltage (*I–V*) relations obtained for $Ca_v2.2$ ($\alpha_{1B} + \beta_{2a} + \alpha_2$–δ) Ca^{2+} channels in the presence and absence of 0.03 μg/ml GLTx for 14 cells. In each case, data obtained with and without GLTx were from the same cell. Control data were normalized to the peak of the *I–V* curve. Note that GLTx induces a leftward shift in the position of the *I–V* curve, as well as a slight inhibition of current activity at depolarized potentials. (**B**) Typical time course of the effect of GLTx on $Ca_v2.2$ channels at a test potential of –10 mV. Inset: representative Ba^{2+} current traces elicited by a step depolarization to –10 mV, before and after application of GLTx, and in response to GLTx plus 300 nM ω-CTx-MVIIA applied after GLTx alone. (**C**) GLTx effect on $Ca_v2.2$ ($\alpha_{1B} + \alpha_2$–δ + β_{2a}) current activity at various test potentials (n = 14). Current activity is increased by GLTx at hyperpolarized voltages, whereas current inhibition is evident at more depolarized potentials. (**D**) Effect of GLTx on the half activation potential of $Ca_v2.2$ channels co-expressed with α_2–δ and one of the four known Ca^{2+}-channel β subunits. The half activation potential was estimated from Boltzmann fits to current–voltage relations such as those shown in (A). Note that GLTx induces a statistically significant shift in half activation potential for each β subunit examined. (**E**) Comparison of the GLTx mediated up-regulation of current activity for the three remaining Ca^{2+}-channel β subunits examined at V_m = –10 mV.

GLTx increases phasic neurotransmitter release at the frog neuromuscular junction by enhancing the quantal content of endplate potentials

Since GLTx was found to shift the current–voltage relationship of $Ca_v2.2$ channels towards more depolarized values, it was of interest to investigate whether the phasic quantal transmitter release was also modified. Therefore the pectoralis propius motor nerve, innervating the frog cutaneous pectoris muscle, was stimulated by single pulses at a low rate (0.2 Hz) and the evoked responses were recorded under conditions in which neurotransmitter release had been reduced by lowering external Ca^{2+} concentration and increasing Mg^{2+} concentration. Upon GLTx application, an increase in endplate potential (EPP) amplitude was detected, which depended on the dose (0.1–0.5 μg/ml) reaching up to 10 times control levels. The quantal content of the evoked responses (estimated by dividing EPP by MEPP amplitude) was clearly enhanced and this sustained effect was reversible by simple wash (Figure 8). At higher concentrations, GLTx induced a blockade of evoked release (data not shown) consistent with the blockade of Ca^{2+} currents observed in patch–clamp experiments at such concentrations. These results clearly demonstrate that GLTx acts presynaptically by modifying the biophysical properties of $Ca_v2.2$ channels, thereby promoting the synchronous recruitment of an increased number of synaptic vesicles for phasic release.

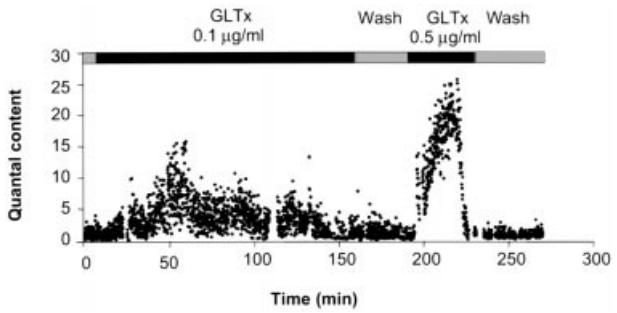

Fig. 8. Effect of GLTx on the mean quantal content of endplate potentials. EPPs evoked by nerve stimulation at 0.2 Hz and MEPPs were recorded from a frog cutaneous pectoris preparation in conditions indicated on the figure. The mean quantal content values were obtained by dividing the amplitude of each EPP by the mean amplitude obtained from 20–50 MEPPs taken randomly within the intervals of stimulation. The resting membrane potential was –90 mV during recordings and the solution bathing the preparation contained 1 mM Ca^{2+} and 6 mM Mg^{2+}.

Discussion

In this study, the purification and characterization of GLTx, a 320 kDa protein stimulating exocytosis of large dense core vesicles in neuroendocrine cells and small synaptic vesicles from frog motor nerve terminals, is described. Involvement of $Ca_v2.2$ was first revealed using selective inhibitors of the various subtypes of VDCC. Moreover, GLTx was found to trigger Ca^{2+} influx in cells

heterologously expressing $Ca_v2.2$ and to interact with this subtype of Ca^{2+} channel by co-immunoprecipitation from synaptosomes.

Previous attempts to isolate the active component responsible for the secretagogue activity of *G.convoluta* venom attributed the activity to a 300 kDa glycoprotein. However, the purity of the final fraction obtained by affinity chromatography using Con A–Sepharose was not refined enough as a number of contaminant proteins were detected (Morel *et al*., 1983). To overcome this problem, additional purification steps have been introduced in this study to eliminate the contaminating glycoproteins before proceeding with the Con A affinity chromatography. Since the active component had been reported to be around 300 kDa, the novel purification protocol was begun by dialysis using a membrane with a 100 kDa cut-off. Following this, ion-exchange and gel filtration steps were introduced prior to the final affinity chromatography. This protocol allowed the purification of three proteins with apparent molecular weights of 320, 148 and 74 kDa. The specific activity typically increased by a factor of more than 1000 during the purification procedure.

Although the ratio of the upper to the lower band differed from preparation to preparation, the level of secretagogue activity exclusively correlated with the abundance of the 320 kDa protein. This was further substantiated by the discovery that mild alkalization caused the selective disappearance of the 320 kDa band and concomitant abolition of the secretagogue activity. As both the 320 and 148 kDa bands were recognized by a monoclonal antibody raised against the active toxin, it is likely that the 148 kDa species is a degradation product of the 320 kDa protein.

The high specific activity of the purified fraction makes GLTx one of the most active toxins yet discovered, working in the picomolar range at the frog NMJ, similar to α-latrotoxin (LTX) from the black widow spider *Latrodectus mactans tredecimguttatus* (Davletov *et al*., 1998; Südhof, 2001) and trachynilysin from the stonefish *Synanceia trachynis* (Meunier *et al*., 2001). The stimulatory activity of LTX mainly depends on the cation-conducting pore formed by LTX, which has been shown to exploit the extracellular domains of two presynaptic proteins to promote its insertion into the plasma membrane (Davletov *et al*., 1998; Volynski *et al*., 2000; Südhof, 2001). An important consequence of this insertion is that LTX effect is irreversible, which is in striking contrast with the equally potent but easily reversible stimulatory effect of GLTx. This strongly suggests that the strategy employed by the two toxins to stimulate neurotransmitter release is different.

Insight into the mode of action of GLTx was provided by the discovery that it had no effect at the mouse EDL nerve–muscle preparation. In fact, GLTx proved to be non-toxic when injected in mice intraperitoneally, even at the high doses used for immunization. In sharp contrast, GLTx potently enhanced spontaneous and evoked quantal transmitter release at the frog NMJ. Despite being widely expressed in the mammalian CNS (Jones *et al*., 1997), $Ca_v2.2$ channels are absent from the adult peripheral motor nerve terminals (Day *et al*., 1997; Katz *et al*., 1997). Thus $Ca_v2.2$ became an obvious candidate for mediating GLTx action. This hypothesis was confirmed by pre-treatment of frog NMJ preparation by ω-CTx-GVIA, which completely prevented GLTx stimulatory effect. The unique involvement of $Ca_v2.2$ was gathered using chromaffin cells, which are known to express three major types of VDCC: Ca_v1, $Ca_v2.1$ and $Ca_v2.2$ (Artalejo *et al*., 1994; Garcia *et al*., 1998). By sequentially inhibiting each of the subtypes, it became clear that only $Ca_v2.2$ was responsible for mediating the toxin's effect.

Attention was then turned to elucidating the mechanism by which GLTx stimulates exocytosis via $Ca_v2.2$ channels. An increase in synaptosomal Ca^{2+} level in response to *G.convoluta* venom has previously been reported (Madeddu *et al*., 1984). Our study suggests that GLTx triggered Ca^{2+} influx through $Ca_v2.2$ channels, which in turn is believed to initiate exocytosis. GLTx triggers an influx of Ca^{2+} sensitive to ω-CTx-GVIA in neuroendocrine cells and transient expression of $Ca_v2.2$ rendered HEK cells responsive to GLTx.

This evidence points to an interaction between GLTx and presynaptic $Ca_v2.2$. $Ca_v2.2$ is comprised of three subunits: α_{1B}, β and α_2–δ. The channel subunit α_{1B} is known to be retained in the ER when not co-expressed with a β auxiliary subunit, the latter being responsible for the targeting of α_{1B} to the plasma membrane by binding to its ER retention signal (Walker and De Waard, 1998; Bichet *et al*., 2000). HEK cells transfected solely with cDNA encoding the α_{1B} subunit of $Ca_v2.2$ were insensitive to GLTx action and sensitivity was conferred only upon co-expression of β_3. This result, together with the reversibility of GLTx stimulatory effect by simple wash, clearly demonstrates that GLTx acts on $Ca_v2.2$ only when expressed at the plasma membrane.

The interaction between $Ca_v2.2$ and GLTx, demonstrated by co-immunoprecipitation using antibodies against GLTx, is particularly interesting in light of the central role played by $Ca_v2.2$ in coordinating several proteins of the secretory apparatus. Indeed, $Ca_v2.2$ has been shown to interact directly with SNARE family members and synaptic vesicle proteins, ensuring that synaptic vesicles are tightly bound to a source of Ca^{2+}. Syntaxin, SNAP-25 and synaptotagmin bind to the synprint region of $Ca_v2.2$, altering the gating properties of $Ca_v2.2$ channel (Catterall, 2000; Jarvis and Zamponi, 2001). Recently, RIM binding proteins were shown to interact with several subtypes of Ca^{2+} channels including $Ca_v2.2$ and to functionally control the strength of secretion (Hibino *et al*., 2002). Future work will address whether GLTx can perturb this equilibrium.

Electrophysiological analysis was performed on transiently transfected HEK tsA-201 cells using patch whole-cell recordings. GLTx induces a leftward shift in the current–voltage relationship in $Ca_v2.2$-expressing cells. As a consequence of this increase in window current, the amplitudes of the elicited Ba^{2+} current increased more than threefold (340 ± 60%) compared with untreated cells upon depolarization from –80 mV to –10 mV. The fact that channels containing the β_3 subunit could undergo a GLTx-evoked increase in the current is consistent with the Ca^{2+} influx detected upon GLTx addition in HEK cells co-expressing α_{1B} and the β_3 rabbit orthologue (Figure 5).

Since GLTx induced an up-regulation of Ca^{2+} currents, we investigated the effect of GLTx on nerve-evoked synchronous quantal transmitter release. We found that the

size of the EPPs was greatly enhanced upon addition of GLTx and remained higher for as long as our experiment lasted. Interestingly, this effect was fully reversible by simple wash. To ascertain that this was a presynaptic effect the quantal content was measured using the ratio method, which confirmed that the number of quanta entering into the composition of EPPs was enhanced by as much as 10 times (Figure 8). In contrast with several neurotoxins that only stimulate spontaneous neurotransmitter release (Schiavo *et al*., 2000), GLTx also enhanced evoked phasic quantal ACh release. This clearly indicates that upon arrival of an action potential, the enhanced elicited Ca^{2+} influx through $Ca_v2.2$ increases the number of synaptic vesicles recruited to build up an EPP.

To date, most compounds found to act selectively upon Ca^{2+} channels are inhibitory (Garcia *et al*., 1998). To the best of our knowledge, only a dihydropyridine derivative (Bay k 8644) has been shown to activate Ca_v1 by favouring the open state of this channel (Hess *et al*., 1984). Ca_v1 is found in skeletal, smooth and cardiac muscles and in neuroendocrine cells (Catterall, 2000; Fisher and Bourques, 2001). In contrast, $Ca_v2.2$ is mostly present in neurons of the CNS and in neurons involved in digestive functions in the PNS (Garcia *et al*., 1998) and is functionally coupled with the exocytic machinery controlling secretion. In this context, GLTx provides a novel and unique tool to study secretion in these neurons and to investigate the functional interaction between $Ca_v2.2$ and the exocytotic machinery at the molecular level.

Materials and methods

Gland dissection

Glycera convoluta specimens were obtained from the Marine Biological Station, Roscoff (France) and the glands were isolated as previously described (Manaranche *et al*., 1980) and stored at –80°C.

Scanning electron microscopy

Glycera convoluta were fixed in 4% paraformaldehyde in Sorensen's phosphate buffer. Fixed animals were dehydrated in ascending ethanol concentrations, washed twice in acetone before critical point drying, mounted and coated with platinum. Samples were examined with a JEOL 5600 field emission scanning electron microscope.

Purification of GLTx

Two hundred glands were thawed, homogenized in 10 mM sodium phosphate buffer (pH 7.2) on ice using a glass–Teflon homogenizer and centrifuged for 5 min at 16 000*g*. The supernatant was kept on ice and the pellet extracted again as above. Supernatants were pooled, clarified by centrifugation (20 min at 16 000*g*) and dialysed for 24 h in a Float A Lyser™ with a 100 kDa molecular weight cut-off (Spectrum, Perbio Science, UK). The dialysed extract was then fractionated by ion-exchange chromatography on a Resource Q column (Amersham Pharmacia Biotech, UK). Bound material was eluted using a linear NaCl concentration gradient (0–1 M in 10 mM sodium phosphate buffer pH 7.2).

Fractions were tested for their ability to stimulate catecholamine release from cultured bovine adrenal chromaffin cells. Active fractions were pooled and concentrated (3 h dialysis 15% (w/v) addition polyethylene glycol (PEG) 20 000 15% (w/v) in a 10 mM sodium phosphate buffer (pH 7.2) before fractionation on a Superdex™ 200 column (Amersham Pharmacia Biotech, UK). Active fractions were pooled and further purified by affinity chromatography on Con A–Sepharose™ (Amersham Pharmacia Biotech, UK). Bound material was eluted with 0.25 M α-methyl-D-mannoside (Sigma, UK) and concentrated by dialysis against 15% PEG as described above. Protein concentration was determined using Bradford protein assay (Biorad, UK). The specific activity was calculated as the percentage of total catecholamine release per milligram of protein (Figure 1E).

Neuromuscular junction preparations

Cutaneous pectoris nerve–muscle preparations were removed from frog (*Rana esculenta*; 25–30 g) and pinned in a Rhodorsil-lined Plexiglas chamber containing a standard frog Ringer solution (115.0 mM NaCl, 2.1 mM KCl, 1.8 mM $CaCl_2$ and 5 mM HEPES–NaOH pH 7.25). To avoid spontaneous contraction, some preparations were pre-treated with tetrodotoxin (TTX, 1 μM). Studies on nerve-evoked quantal transmitter release were performed in solutions containing low Ca^{2+} (1 mM) and high Mg^{2+} (6 mM) concentrations. The EDL muscle was removed from adult Swiss-Webster mice (25–30 g) and pinned in a similar Rhodorsil-lined chamber containing continuously oxygenated Krebs–Ringer solution (151 mM NaCl, 5 mM KCl, 1 mM $MgCl_2$, 2 mM $CaCl_2$, 11 mM glucose and 5 mM HEPES–NaOH pH 7.4).

Cell culture and transfection

Exponentially growing human embryonic kidney (HEK 296 or HEK tsa-201) cells, seeded at 2×10^6 cells/10 cm dish, were transfected by calcium phosphate (Feng *et al*., 2001a) for patch–clamp experiments and electroporation for monitoring Ca^{2+} variations (400 V; infinity resistance, 125 μF) using a Gene Electropulser II (BioRad, CA) with 10 μg of total DNA using equimolar ratios of expression constructs encoding the following subunits of VDCC: α_{1A} (Mori *et al*., 1991), α_{1B} (Fujita *et al*., 1993), α_2–δ (Kim *et al*., 1992), β_3 (Witcher *et al*., 1993), β_{1b}, β_{2a} and β_4 (Feng *et al*., 2001b).

Electrophysiological recordings

MEPPs and EPPs were recorded at room temperature (22°C) with an intracellular glass capillary microelectrode filled with 3 M KCl (8–12 Ω) using conventional techniques. The motor nerve of the isolated NMJ preparation was stimulated via a suction microelectrode. After amplification, electrical signals were digitized, displayed on an oscilloscope and simultaneously recorded on videotape with the aid of a modified digital audio processor (Sony PCM 701 ES) and a videocassette recorder (Sony SLC 9F). Data were collected and analysed with SCAN, software kindly provided by Dr John Dempster (University of Strathclyde, UK) running on a PC equipped with an analogue–digital converter (Model DT2821, Data Translation, MA).

Whole-cell patch–clamp recordings were performed as described previously (Feng *et al*., 2001b). GLTx dissolved in the recording solution [5 mM $BaCl_2$, 1 mM $MgCl_2$, 10 mM HEPES, 40 mM TEA-Cl, 10 mM glucose, 97.5 mM CsCl (pH 7.2 adjusted with TEA-OH)] was perfused onto the cells using a gravity-driven perfusion system. Current–voltage relations exported from Clampfit (Axon Instruments, CA) were fitted with Sigmaplot 4.0 (Jandel Scientific, CA) using the Boltzmann relation

$$I = \{1/(1 + \exp(-(V_m - V_a)/k))\}\{G(V_m - E_{rev})\}$$

where V_m is the test potential, V_a is the potential at which half of the channels are activated, G is the maximal slope conductance, E_{rev} is the reversal potential and k is the slope of the activation curve.

Culture of bovine adrenal chromaffin cells, and stimulation and quantification of catecholamine secretion

Chromaffin cells were prepared from bovine adrenal glands and maintained as primary cultures in 24-well plates (Nunc, UK) as previously described (Meunier *et al*., 2000). Chromaffin cells were briefly washed once with buffer A (145 mM NaCl, 5 mM KCl, 1.2 mM Na_2HPO_4, 10 mM glucose and 20 mM HEPES–NaOH pH 7.4), and processed as stated in the figure legends. Aliquots of the medium were taken at the end of each experiment and cells were lysed with 1% (v/v) Triton X-100 (Sigma, UK). Both sets of samples were assayed fluorimetrically for catecholamine content, and the amounts released were expressed as a percentage of the total amount of catecholamine present in the cells. Plotted data are representative of at least four independent experiments, each carried out in quadruplicate.

Intracellular Ca^{2+} imaging

Chromaffin and HEK cells cultured on glass bottom (no. 1.5) dishes (MatTek Corporation, MA) coated with poly-L-lysine (0.1 mg/ml; Sigma, UK) were loaded with the acetoxymethyl ester form of fura-2 or fluo-3 [5 μM with 0.02% pluronic acid (w/v) for 45 min at 37°C in the dark] in Buffer A or Hanks' buffer (136 mM NaCl, 5.36 mM KCl, 0.81 mM $MgCl_2$, 1.26 mM $CaCl_2$, 0.44 mM KH_2PO_4, 0.81 mM $MgSO_4$, 0.42 mM Na_2HPO_4, 11 mM glucose and 20 mM HEPES–NaOH pH 7.4), respectively. After washing and incubation at 37°C for 15 min, the dishes were placed in an environmental chamber (37°C) on the stage of a confocal (LSM510, Zeiss, Germany) or epifluorescent microscope

(Diaphot 300, Nikon, UK) equipped with Plan Fluor 40×, 60× or 100×, N.A. 1.3 oil-immersion lenses. For confocal Ca^{2+} imaging, fluo-3-loaded cells were processed as previously described but using the above-mentioned objectives (Meunier *et al*., 2000).

For ratiometric measurement of intracellular Ca^{2+}, fura-2-loaded cells were alternatively excited through 340 and 380 nm filters and images were acquired using a cooled CCD camera (Orca I, Hamamatsu, Japan) controlled by AQM2000 software (Kinetic Imaging, UK). Images were taken at 5 s intervals and ratios obtained using Lucida (v.4.0; Kinetic Imaging, UK).

The index of the fluorescence variations $\Delta F/F_0$ used to quantify the relative changes of intracellular Ca^{2+} was calculated as follows:

$$\Delta F/F_0 = [(f_{340}/f_{380})_i - (f_{340}/f_{380})_{max}] / (f_{340}/f_{380})_i$$

where $(f_{340}/f_{380})_i$ is the initial fluorescence ratio measured before application of the relevant drug or toxin and $(f_{340}/f_{380})_{max}$ is the maximal fluorescence ratio taken at the peak of the effect.

Preparation of anti-GLTx monoclonal antibodies

Balb/c mice were immunized by intraperitoneal injections (every 4 weeks) of 50 μg of purified GLTx. Serum and hybridoma supernatants were tested for their ability to inhibit GLTx secretagogue activity in chromaffin cells. The clone 4G9 was singled out for its ability to partially inhibit the stimulatory activity of both the venom and purified GLTx and to recognize purified GLTx in dot-blots and western blotting.

Immunoprecipitation and western blotting

Crude synaptosomes were prepared from rat brain cortex following the method of Huttner *et al*. (1983) with minor variations. Seventy milligrams of synaptic plasma membranes (LP1) were solubilized in 10 mM HEPES–NaOH pH 7.4 containing protease inhibitors (Pefabloc, Roche Boehringer Mannheim, Germany) and 4% octyl-β-D-glucopyranoside (OG) for 1 h. In some experiments, 5 mg of LP1 were pre-incubated for 1–2 h with [^{125}I]ω-CTx-GVIA (0.5 μCi; NEN, UK), washed twice by ultracentrifugation and solubilized as described above. Detergent-free buffer was added to dilute the OG to a final concentration of 1.2% and the insoluble material was removed by centrifugation. The extract was pre-incubated for 2–4 h at 4°C with Protein G–Sepharose (Roche Boehringer Mannheim, Germany) coupled or not with 4G9 monoclonal antibodies with or without pre-binding of GLTx for 2 h (at concentrations indicated in Figure 6).

Protein samples were heated at 100°C for 3 min in 2% SDS sample buffer, and proteins were resolved in 8% or 12% SDS–polyacrylamide gels. Proteins were transferred (200 mM glycine, 25 mM Tris–OH, 10% methanol) to nitrocellulose membrane (0.2 μm; Schleicher and Schuell, UK), blocked in TBST (20 mM Tris–HCl pH 7.6, 137 mM NaCl, 0.05% Tween 20) containing 1% ovalbumine (w/v) and 1% polyvinylpyrrolidone (w/v) and probed for 2 h with indicated antibodies diluted in blocking solution (mouse anti-GLTx, 0.1 μg/ml; rabbit anti-α_{1B}, 8 μg/ml; Cambridge Bioscience, UK). After washing three times with TBST, the membranes were incubated with the appropriate HRP-conjugated secondary antibody in blocking solution (1:2000) for 1 h, washed and revealed by enhanced chemoluminescence (ECL; Amersham Pharmacia Biotech, UK).

Drugs and toxins

Aga TK (Alomone, Israel); ω-CTx-GVIA (Calbiochem, UK); ω-CTx-MVIIA (Alomone, Israel); Verapamil (D600) (Sigma, UK); TTX (Sigma, UK); fluo-3/AM and fura-2/AM (Molecular Probes, The Netherlands).

Statistical analysis

Statistical analysis was performed using Student's *t*-test (two-tailed, paired or unpaired depending on the experimental protocol). Values are expressed as mean ± SEM and data were considered significant (*) at $P < 0.01$.

Acknowledgements

We thank S.L.Osborne for LP1 preparation and excellent suggestions, S.Tooze, D.Shima and M.Seagar for critical reading of the manuscript, S.Gschmeissner for electron microscopy and B.Adams for the kind gift of the plasmids encoding Ca^{2+} channels. This work was supported by Cancer Research UK (F.A.M. and G.S.), by the Direction des Systemes de Forces et de la Prospective (J.M.), by an operating grant from the Heart and Stroke Foundation of Alberta and the Northwest Territories (G.W.Z.) and by travel grant BC 00156SE from the British Council (F.A.M., J.M. and G.S.). Z.P.F. holds postdoctoral awards from the Canadian Institutes of Health Research (CIHR) and the Heart and Stroke Foundation of Canada. G.W.Z. is a CIHR Investigator and a Senior Scholar of the Alberta Heritage Foundation for Medical Research.

References

Artalejo,C.R., Adams,M.E. and Fox,A.P. (1994) Three types of Ca^{2+} channel trigger secretion with different efficacies in chromaffin cells. *Nature*, **367**, 72–6.

Bichet,D., Cornet,V., Geib,S., Carlier,E., Volsen,S., Hoshi,T., Mori,Y. and De Waard,M. (2000) The I–II loop of the Ca^{2+} channel α_1 subunit contains an endoplasmic reticulum retention signal antagonized by the β subunit. *Neuron*, **25**, 177–90.

Catterall,W.A. (2000) Structure and regulation of voltage-gated Ca^{2+} channels. *Annu. Rev. Cell. Dev. Biol.*, **16**, 521–55.

Davletov,B.A., Meunier,F.A., Ashton,A.C., Matsushita,H., Hirst,W.D., Lelianova,V.G., Wilkin,G.P., Dolly,J.O. and Ushkaryov,Y.A. (1998) Vesicle exocytosis stimulated by α-latrotoxin is mediated by latrophilin and requires both external and stored Ca^{2+}. *EMBO J.*, **17**, 3909–20.

Day,N.C., Wood,S.J., Ince,P.G., Volsen,S.G., Smith,W., Slater,C.R. and Shaw,P.J. (1997) Differential localization of voltage-dependent Ca^{2+} channel α_1 subunits at the human and rat neuromuscular junction. *J. Neurosci.*, **17**, 6226–35.

Feng,Z.P., Arnot,M.I., Doering,C.J. and Zamponi,G.W. (2001a) Calcium channel β subunits differentially regulate the inhibition of N-type channels by individual Gβ isoforms. *J. Biol. Chem.*, **276**, 45051–8.

Feng,Z.P., Hamid,J., Doering,C., Bosey,G.M., Snutch,T.P., Zamponi, G.W. (2001b) Residue Gly1326 of the N-type calcium channel α_{1B} subunit controls reversibility of ω-conotoxin GVIA and MVIIA block. *J. Biol. Chem.*, **276**, 15728–35.

Fisher,T.E. and Bourques,C.W. (2001) The function of Ca^{2+} channels subtypes in exocytic secretion: new perspectives from synaptic and non-synaptic release. *Prog. Biophys. Mol. Biol.*, **77**, 269–303.

Fujita,Y. *et al*. (1993) Primary structure and functional expression of the ω-conotoxin-sensitive N-type Ca^{2+} channel from rabbit brain. *Neuron*, **10**, 585–98.

Garcia,A.G., Albillos,A., Cano-Abad,M.F., Garcia-Palomero,E., Hernandez-Guijo,M., Herrero,C.J., Lomax,R.B. and Gandia,L. (1998) Ca^{2+} channels for exocytosis in chromaffin cells. *Adv. Pharmacol.*, **42**, 91–4.

Hess,P., Lansman,J.B. and Tsien,R.W. (1984) Different modes of Ca^{2+} channel gating behaviour favoured by dihydropyridine Ca^{2+} agonists and antagonists. *Nature*, **311**, 538–544.

Hibino,H., Pironkova,R., Onwumere,O., Vologodskaia,M., Hudspeth, A.J. and Lesage,F. (2002) RIM binding proteins (RBPs) couple Rab3-interacting molecules (RIMs) to voltage-gated Ca^{2+} channels. *Neuron*, **34**, 411–423.

Huttner,W.B., Schiebler,W., Greengard,P. and De Camilli,P. (1983) Synapsin I (protein I) a nerve terminal-specific phosphoprotein. III. Its association with synaptic vesicles studied in a highly purified synaptic vesicle preparation. *J. Cell Biol.*, **96**, 1374–1388.

Jarvis,S.E. and Zamponi,G.W. (2001) Distinct molecular determinants govern syntaxin 1A-mediated inactivation and G-protein inhibition of N-type calcium channels. *J. Neurosci.*, **21**, 2939–2948.

Jones,O.T., Bernstein,G.M., Jones,E.J., Jugloff,D.G., Law,M., Wong,W. and Mills,L.R. (1997) N-type Ca^{2+} channels in the developing rat hippocampus: subunit, complex, and regional expression. *J. Neurosci.*, **17**, 6152–6164.

Katz,E., Protti,D.A., Ferro,P.A., Rosato Siri,M.D. and Uchitel,O.D. (1997) Effects of Ca^{2+} channel blocker neurotoxins on transmitter release and presynaptic currents at the mouse neuromuscular junction. *Br. J. Pharmacol.*, **121**, 1531–1540.

Kim,H.L., Kim,H., Lee,P., King,R.G. and Chin,H. (1992). Rat brain expresses an alternatively spliced form of the dihydropyridine-sensitive L-type Ca^{2+} channel α_2 subunit. *Proc. Natl Acad. Sci. USA*, **89**, 3251–3255.

Lichtenegger,H.C., Schöberl,T., Bartl,M.H., Waite,H. and Stucky,G. (2002) High abrasion resistance with sparse mineralization: copper biomineral in worm jaws. *Science*, **298**, 389–392.

Madeddu,L., Meldolesi,J., Pozzan,T., Cardona Sanclemente,L.E. and Bon,C. (1984) α-Latrotoxin and glycerotoxin differ in target specificity and in the mechanism of their neurotransmitter releasing action. *Neuroscience*, **12**, 939–949.

Manaranche,R., Thieffry,M. and Israel,M. (1980) Effect of the venom of

Glycera convoluta on the spontaneous quantal release of transmitter. *J. Cell Biol.*, **85**, 446–458.

Meunier,F.A., Mattei,C., Chameau,P., Lawrence,G., Colasante,C., Kreger,A.S., Dolly,J.O. and Molgó,J. (2000) Trachynilysin mediates SNARE-dependent release of catecholamines from chromaffin cells via external and stored Ca^{2+}. *J. Cell Sci.*, **113**, 1119–1125.

Meunier,F.A., Ouanounou,G., Mattei,C., Chameau,P., Colasante,C., Ushkaryov,Y.A., Dolly,J.O., Kreger,A.S. and Molgó,J. (2001) Secretagogue activity of trachynilysin, a neurotoxic protein in stonefish (*Synanceia trachynis*) venom. In Massaro,E.J. (ed.), *Neurotoxicity of Synthetized and Natural Chemical Substances*. Humana Press, Totowa, NJ, USA, Vol. 1, pp. 595–615.

Morel,N., Thieffry,M. and Manaranche,R. (1983) Binding of a *Glycera convoluta* neurotoxin to cholinergic nerve terminal plasma membranes. *J. Cell Biol.*, **97**, 1737–1744.

Mori,Y. *et al*. (1991) Primary structure and functional expression from complementary DNA of a brain calcium channel. *Nature*, **350**, 398–402.

Olivera,B.M., Gray,W.R., Zeikus,R., McIntosh,J.M., Varga,J., Rivier,J., de Santos,V. and Cruz,L.J. (1985) Peptide neurotoxins from fish-hunting cone snails. *Science*, **230**, 1338–1343.

Olivera,B.M., Cruz,L.J. and Yoshikami,D. (1999) Effects of *Conus* peptides on the behavior of mice. *Curr. Opin. Neurobiol.*, **9**, 772–777.

Robitaille,R., Adler,E.M. and Charlton,M.P. (1990) Strategic location of calcium channels at transmitter release sites of frog neuromuscular synapses. *Neuron*, **5**, 773–779.

Schiavo,G., Matteoli,M., Montecucco,C. (2000) Neurotoxins affecting neuroexocytosis. *Physiol. Rev.*, **80**, 717–766.

Südhof,T.C. (2001) α-Latrotoxin and its receptors: neurexins and CIRL/latrophilins. *Annu. Rev. Neurosci.*, **24**, 933–962.

Volynski,K.E. *et al*. (2000) Latrophilin, neurexin, and their signaling-deficient mutants facilitate α-latrotoxin insertion into membranes but are not involved in pore formation. *J. Biol. Chem.*, **275**, 41175–41183.

Walker,D. and De Waard,M. (1998) Subunit interaction sites in voltage-dependent Ca^{2+} channels: role in channel function. *Trends Neurosci.*, **21**, 148–154.

Witcher,D.R., De Waard,M., Sakamoto,J., Franzini-Armstrong,C., Pragnell,M., Kahl,S.D. and Campbell,K.P. (1993) Subunit identification and reconstitution of the N-type Ca^{2+} channel complex purified from brain. *Science*, **261**, 486–489.

Received May 29, 2002; revised October 23, 2002; accepted October 24, 2002